SPE 159532-PP

An Innovative Static Modeling Approach to handle a Complex Giant Mature Field within a Compressed Timeframe ; A Case Study of the Baram Oil Field, Offshore Sarawak, East Malaysia.

Agus Izudin Latief, ROXAR; Ahmad Idriszuldin Ridzuan, PETRONAS; Paul Andrew Faehrmann, SHELL; Alister MacDonald, ROXAR; Wardah Arina Nasir, PETRONAS; Gozali Rahman, ROXAR; Mohd Elzrey Rahman, PETRONAS.

This paper was prepared for presentation at the SPE Asia Pacific Oil and Gas Conference and Exhibition held in Perth, Australia, 22–24 October 2012.

Abstract

Baram is a giant mature field situated, offshore Sarawak Malaysia. Reservoirs consist of an approximately 7000 ft thick-stacked sequence of shallow marine sands, distributed in excess of 200 zones. The field is extensively faulted. Early Growth faulting followed by a later compressional phase has led to complex fault geometries. The field has been producing for over 40 years and presently has 175 wells.

Although the reservoirs are generally of good quality, the field currently has relatively low production rates, a low recovery factor, and a significant amount of remaining reserves. The geological complexity poses a key challenge, and a robust static reservoir model is a prerequisite for efficient reservoir management and for identifying viable Improved Oil Recovery (IOR) measures.

Static models of the Baram field had previously been constructed. This modelling took in excess two years to complete and the models were segmented into 10 pieces, as technology during this period was unable to tackle complex fault geometries. Due to the results of the static / dynamic modelling being insufficiently robust when tested during a drilling campaign in 2009, the decision was made to remodel.

The Baram subsurface team was challenged with building a static model which could be used for field management and IOR /EOR process selection and optimization within a six month timeframe. This is to allow for early investment decisions and an accelerated reversal of production decline. The key aspects of the fixed timeframe static model construction are described below. They consist of:

1. The subdivision of the field into independent models.
2. The utilization of a modern algorithm to model complex fault geometry.
3. Nested stratigraphic modeling.
4. Parallel property modeling and the re-combining of results into a single simulation grid to enable integrated reservoir simulation.

A full focus on the importance of the timeline and early investment, plus the adoption of a variety of strategic project management measures and use of "state of the art" modeling technology can allow fit-for-purpose static models to be delivered on time.

Introduction

The Baram Field, situated 30 km northwest of Lutong, Malaysia, is one of nine fields in the Baram Delta Operations (BDO) area offshore Miri, Sarawak. It is located in approximately 60-200 ft water depth. The field is divided into two main parts: Baram North and South, which are separated by a major growth fault striking in the E-W direction. Baram North itself is

divided further into Baram A, B, and saddle area. Baram B represents hydrocarbon accumulation at the northwestern part of the field and is smaller in terms of size and number of wells compared to Baram A, which is located at the northeastern side. The saddle area has been appraised and is confirmed to have no hydrocarbon finding. Consequently no common fluid contacts were identified between Baram A and B. A complete outline of the field can be seen in **Figure 1**.

The depocenter of the Baram field was developed during Late Eocene, and from early Middle Miocene onwards and was characterized by regressive phases of clastic sedimentation. The sedimentation cycle in the area is the result of interplay between tectonic, sea level fluctuation, and also the rate of sediment supply. The Baram structure is formed on an active continental margin with two main deformation types identified:

- An Extensional event, during middle to lower Miocene, which produced a WSW-ENE trending growth fault.
- A Compressional event induced by strike slip movement during Pliocene, which created folding and inverted some of the existing faults. Generally, wrench induced deformation effect decreases basinward. This compressional event also made crestal collapse faults at the crest of positive structures, which complicate lateral compartment at shallower sections.

There are 13 reservoir sequences identified in Baram Field and approximately 90 major reservoir units. In total, reservoir thickness is about 7000 ft with major hydrocarbon accumulation belonging to the Cycle V and VI of the Upper Miocene and Pliocene ages. Reservoirs are highly compartmentalized, vertically by interbedded shale, and laterally by faults. However, along with increasing differential pressure after production, some of seals may have broken and started to allow fluid transfer from one compartment to another. The limited reservoir surveillance data, comingling of reservoir production and minimal PLT monitoring presents difficulties in implementing proper reservoir management. Hence, production allocation is only based on permeability thickness (Kh) proportion. These facts pose a real challenge for both static and dynamic modeling.

The naming convention for reservoirs, fault blocks, and any other related information in this paper is meant for reference only and does not represent actual names. The following are hydrocarbon bearing intervals starting from the shallowest, i.e: A1, A2, A3, A4, A5, A6, A7, A8, A9, A10 (see **Figure 2**). Due to their complexity, it is believed that a thorough review, with an integrated perspective, will reveal the significant potential of remaining hydrocarbons. It is a reasonable assumption considering an inverse relation between reservoir quality and current recovery factors. The realization of this hydrocarbon potential trigger a Baram Field revitalization project which is part of a major IOR/EOR campaign to rejuvenate mature fields in Malaysia.

The Baram Field has become one of the main focuses, considering the size of its potential. The project timeline has been setup and accordingly, the integrated static model has to be finished by end of 2011, or within a six months time frame to be aligned with the overall IOR/EOR project timeframe. It is a huge task to be accomplished, considering the field's size and complexity.

Methodology

The integrated static model of Baram is initiated by building a single structural framework for the whole field. By doing this, the consistency of the horizon and fault framework for the whole field is maintained, regardless of the location of the sector model grid extracted from the framework. Moving forward, to ensure static model completion within the timeframe, several strategic measures are taken as follows:

1. Subdivision of the field into independent models.
2. Utilization of modern algorithm to model complex fault geometry.
3. Nested stratigraphic modeling.
4. Parallel property modeling and the re-combining of the results into a single simulation grid to enable integrated reservoir simulation.

1. Subdivision of the field into independent models. There is a static model of Baram Field which was constructed in 2006. However, the Baram Field was segmented into 10 sector models. Consequently, some lateral inter-fault blocks pressure and fluid communication could not be simulated. Several zones which are commingled also need to be simulated separately due to the sector models approach. This problem was realized during model construction, but fault geometry complexities hampered efforts to combine the sector models to achieve integrated simulation. The large vertical extent of the Baram Field reservoirs also becomes a predicament as the shapes of fault intersections become very complex.

Technology has evolved since then with an improved fault modeling algorithm enabling any kind of fault geometries and relations to be modeled easily. It makes the creation of a single integrated model for the whole Baram Field possible, solving previous problems. Initially, a "Master" structural model of the entire field was constructed. It become apparent however, that working with one giant model would slow down the project delivery due to slow computing time. It was therefore decided to

aim for four sub models as the final product which:

a) included all the most important reservoirs
b) displayed insignificant pressure communication
c) were not commingled

The criteria set up for the sub-models split serves the purpose for integrated reservoir simulation. The sub-models are started by splitting the Baram North model into Baram A and B. For the whole Baram field, A10 reservoirs are never commingled with other shallow zones. Hence, the Baram A model is then divided further into A5 - A10 models while Baram B is split into A8 - A10 models.

2. Utilization of a modern algorithm to model complex fault geometry. A modern algorithm for modeling the complex fault geometries in the Baram field was used. This algorithm is fully automated, data driven and able to model complex geometries that would not have been possible using more conventional pillar gridding or binary methods.

The algorithm consists of a modified binary approach [see Hoffman et al. (2008)]. It builds faults using 'triangularized surfaces' instead of 'pillars' in a pillar base method. The utilization of surfaces to model faults provides flexibility and removes the restrictions of the pillar based method. Faults no longer have to be terminated by others, gentle dipping fault will not result in dipping grid pillars, and complex fault interactions (crossing faults, half-lambda faults, half-Y faults, and other similar geometries) are no longer an issue.

The usage of surfaces to model faults is adopted from the binary approach. However, the conventional binary method requires a strict definition of foot-wall and hanging-wall sides for each fault. Therefore, partial fault penetration could not be modeled. The current method describes a compound fault relationship which identifies each section of faults truncated by others. The combination (surface-based faults and a compound relationship description) has generated a very flexible fault modeling algorithm. All challenging fault geometries in Baram have successfully been modeled and several examples are shown in **Figure 3**.

3. Nested stratigraphic modeling. The stratigraphic horizons were modeled using a three level nested approach. The first level included the seismically defined horizons and the 2nd level included individual or combined "parasequences". These models were very quick to run and allowed the optimization of the large-scale geometry before the time consuming 3rd level stratigraphic modeling of individual reservoirs was carried out. The nested horizon modeling framework is illustrated in **Figure 4**.

The nested process also makes the QC process easier and more efficient. It is started with only seismic interpreted horizons, and involves well picks. After the framework is considered to have good quality, it is frozen and used as a basis for generating the next level detail of the horizon model. For simple models, the advantage of doing horizon modeling in such way is not substantial. However, when it comes to modeling a giant field, focused directly on over thirty-thousand well picks and hundreds of zones at once, it can be an extremely tedious and error prone process.

In addition to the nested approach, the Baram horizon model no longer implements continuous surfaces as inputs. Instead, surfaces are defined uniquely in fault blocks which address cases of reverse faults or requirement to have multi-z description easily. A fault block here refers to a software description of the area/block in respect of surrounding faults and is not necessarily a closed system, often relating to fault extrapolation. It is more a result of a software artificial intelligent algorithm and has no relation with the geology.

4. Parallel property modeling. To accommodate the tight project timeframes, an innovative project management approach was adopted during the property modeling phase. The model was split into key stratigraphic intervals to enable the parallel execution of the property population workflow. Several Geomodellers worked concurrently during this process, shortening the timeframe, improving the QC process, and maintaining a good quality model as a result. The work process is illustrated in **Figure 5**. After the parallel property modeling, the models were re-combined for integrated reservoir simulation.

There are significant associated risks with this approach, i.e. :

- Model inconsistency due to some level of subjective interpretation involved during the property modeling.
- Substantial differences of duration required between geomodellers to complete tasks and which would obstruct the generation of the integrated model on schedule.

The risks mainly derive from differing knowledge and capability levels of the team members, which is actually a common theme of most sub-surface projects. To overcome this problem, a universal, fit for purpose property modeling technique was

designed. The main idea was to find common geological aspects of modeled reservoirs and a consistent way of describing reservoir heterogeneity. All the ideas were then manifested in a high level workflow as outlined in **Figure 6**. The workflow served as a guideline and milestone check during the property modeling process, and hence consistent results both from modeling and the timeframe perspective were attainable. A detailed description of the workflow together with the underlying concept is elaborated below.

Common Geological Aspect.

The modeled reservoirs cover the A5, A6, A7, A8, A9, and A10 intervals. Out of the interval modeled, only a limited core was acquired over sections of the A6, A7, and A10 reservoirs. Despite the limited coverage, the stratigraphic development intersected provided a good overview of the depositional system's evolution.

The core in the A10 reservoirs indicate a predominantly shoreface dominated depositional system with some minor tide dominated intervals. This is marked by coarsening upward features together with the presence of swaley cross-stratification, hummocky cross-stratification and lesser heterogeneous sandstone. Cores in A6 and A7 reservoirs similarly suggest deposition occurred within a near shore shallow marine to shoreline complex, consisting of a shoreface and tidal channel depositional environment. Log signatures support the interpretation very well with a commonly developed coarsening upward log motif. All the inspections align with a regional concept, whereby the reservoirs being modeled were deposited in an overall regressive event, particularly over the A10 reservoir interval. The overall control of deposition is related to depositional provenance, basin orientation and the underlying structural fabric. Synthesis of the Baram reservoir depositional concept is then constructed and outlined in **Figure 7**. A common theme for the modeled reservoirs is straight forward, i.e : a shoreface depositional system. The main character of the shoreface deposit is then reflected during selection of the property modeling technique.

Reservoir Heterogeneity Description.

The heterogeneity description of the reservoir is a critical part in every modeling exercise as it has direct impact on hydrocarbon volumetric and reservoir flow character. The common approach is where either the geologist and/or sedimentologist review cores and log signatures generate facies interpretation out of the data. This is important, especially in the complex depositional setting i.e. : fluvial and turbidite environments where each facies unit will have a distinct geometry. However, the approach takes time and the quality of the result is highly dependent on the knowledge and experience of the interpreter.

The Baram property model was scheduled to be finished within two months. The adoption of the afore mentioned approach in the Baram case was not considered appropriate, however, due to the following factors:

- Four geomodellers with differing level of knowledge and experience working concurrently on the project. The establishment of geological facies interpretation will therefore likely yield an inconsistent framework unless integrated.
- The large number of wells data (150 +) and reservoir zones (~ 200). The detailed reservoir specific geological facies interpretation will take excessive time and delay project completion.

The best approach for Baram and similar studies is therefore to utilize quantitative lithology classification as it offers consistency and an efficient timeline. In principal, there are two ways that lithology classification has been widely adopted to conduct such classification:

a. Petrophysical based Classification.
This is where reservoir petrophysical properties, such as volume of clay (Vcl), porosity (Φ), and permeability (K), are used directly, through a specific mathematical function, to create a lithological classification. The properties could be used independently or concurrently, depending on the lithological complexity to be described. An example of such classification can be found in the following reference [see Silva et al.(2002) and Guo et al.(2005)].

b. Artificial intelligence classification.
In this approach, petrophysical properties are also used as a basis of lithology classification. However, rather than putting them in a general equation, the properties variation are analyzed against, (usually) core lithological evaluation, to come up with specific trends which can then be applied to predict lithological class in the un-cored intervals. There are differing methodologies that have historically been used, i.e : fuzzy logic [see Cuddy (1998)], neural network [see Bhatt and Bhelle (2002) and Benzaoui et al. (2009)]. The comparison of several artificial intelligent methods also have been evaluated [see Dubois et al.(2005)]. The reliability of these methods will be highly dependent on core data coverage since it serves as a training ground for the algorithm to evaluate lithological heterogeneity.

Artificial intelligence classification is considered unreliable in the Baram field, due to the limited core coverage providing insufficient learning. The lithology classification is instead based on a density-neutron crossplot and sand-silt-clay petrophysical interpretation model. The lithology class is described as rock type and tied back to the core lithological interpretation. From the cores there are eight distinct elements described which are then grouped into four rock types. Rock Type 1 corresponds to the best reservoir quality followed by Rock Type 2 and so forth (**Figure 8**).

A reasonable match is observed when comparing log-derived Rock Type to the core interpreted Rock Type (**Figure 9**). Hence, it was assumed that the classification could be propagated towards all modeled reservoir intervals. It is important to note that while the Rock Type may reasonably describe petrophysical variation, it does not necessarily relate to the diagenetic facies distribution, in this case : upper, middle, and lower shoreface.

Property Modeling Approach.

Using the above synthesis of geology and reservoir heterogeneity, a common, fit for purpose property modeling workflow was set up. Porosity, both effective and total, were populated at first, guided by shoreface deposit heterogeneity patterns and the underlying depositional model concept. As discussed previously, Rock Type is not necessarily related to genetic unit facies, hence Rock Type is not directly modeled as a pre-cursor of petrophysical modeling. In addition, the gradual nature of the shoreface deposit areal transition does not strictly require facies to be modeled as guidance for petrophysical properties population.

Key characters of shoreface deposits are good sand continuity along the shoreline with more rapid sand quality variation along the depositional dip. A shoreface genetic unit is usually described as a belt with the following vertical succession: Lower, Middle and Upper shoreface. Upper shoreface is proximal to shoreline and sediment provenance with good reservoir quality in general while Lower shoreface is more distal and has poorer reservoir quality. Middle shoreface is simply the transition zone in between.

In the modeling workflow, proximal to distal reservoir quality degradation by extracting lateral porosity trend from well data is illustrated in **Figure 11**. The dominant observed azimuth is N 165 E with gradient 1 %/1000 ft for Baram-B and N 175 E with gradient of 0.6 %/1000 ft for Baram-A respectively. This is pretty well aligned with regional knowledge that depositional direction is approximately perpendicular to the paleo-shoreline. The paleo shoreline trend itself is coincident with the NNE-WSW regional growth fault (**Figure 13**). This lateral trend, unique for each modeled horizon, is combined with a regional compactional trend (**Figure 12**) guiding porosity population.

To proceed into the permeability and saturation model, lithological class becomes important. Different lithological classes will have different poro-perm and saturation height relationships. To establish the lithological class in the 3D model, previously populated effective porosity (Phie) and total porosity (Phit) were used to create rock type (RT) trend, taking advantage of Phit-Phie-RT clusters at the well location. The RT trend was then used as a secondary parameter during RT population using Sequential Indicator Simulation (SIS).

Once the RT model is established, permeability is populated using poro-perm function [see Choo (2010)] which specifies for each rock type. Doing this alone, will heavily restrict the permeability range according to the function and will not reproduce cloud variation as shown by well data. In addition, at the well location, the permeability from the 3D model will not be exactly similar to log permeability, since the function itself is basically only a best-fit line in the poro-perm cloud.

To overcome this weakness, cloud transform [see Aly et al. (1999)] was conducted after the poro-perm function implementation. This has two purposes: reproducing permeability log values at well locations in the 3D model and generating poro-perm cloud for more realistic permeability variations against total porosity as shown by logs and routine core analysis (RCA) data (see **Figure 10**). The Combination (Poro-perm function and cloud transform) produce very encouraging results (see **Figure 14**). With only poro-perm function, there is practically no permeability variation for a Phit value in each rock type as demonstrated by the green lines. Cloud transform adoption generates the variation and reproduces the poro-perm cloud shown by logs data. The crossplot of the poro-perm 3D model is shown as points with different color according to rock type.

Overall, the property model result reflects the geology setting very well and the anisotropy of the shoreface environment is also very well represented. Petrophysical properties show a very good continuity along shoreline. Still, the imposed trend honors geological observation at the well location, as demonstrated by some disturbed trend at the northeastern side of Baram-A area (**Figure 15**) as result of tidal process intervention. This tidal process signal is commonly observed towards shallow reservoirs as expected by the regional geology inference.

Saturation Modeling.

Saturation was modeled using modified leverett J-function. The equation has been tested at well level and has achieved a satisfactory match when compared with Sw from log. The main challenge during the exercise is to incorporate large amounts of fluid contact information dispersed in Baram Field. In total, there are about one thousand reservoir compartments in Baram with each of them having individual contacts, mostly of the three phase system (Gas-Oil-Water).

Considering the number of compartments, fluid contact determination is a very tedious and challenging process. Pressure plots cannot be used as only 12 Repeat Formation Tester (RFT) points are considered as having initial pressure information which spreads across 7000 ft of reservoir sections. Sand-shale intercalations with average sand thickness of only 15-20 ft generally preclude any amplitude anomaly (flat spot). Therefore, fluid contact determination relies fully on logs, saturation height function, and the statistical approach as a last resort. The order of event priority and the respective fluid contact determination could be referred in **Table 1**. The table is tabulated in terms of priority where if Oil Water Contact (OWC) is observed, this OWC will be extrapolated to Free Water Level (FWL) using Saturation Height Function (SHF). If no contacts are observed and good saturation profile from logs was observed, we tried to estimate the FWL by fitting the Sw curves. If matching between SHF and Sw log is poor, then we use the halfway method to determine the FWL between Oil Down To (ODT) and Water Up To (WUT), provided that the distance between ODT and WUT is less than 30 ft. If else fails, then we use Gas Oil Contact (GOC) + average oil column height to determine the FWL. About 82% of the Baram FWL was determined from SHF curve fittings.

For GOC determination, if GOC was observed, then we used GOC. If no GOC was observed and only Gas Down To (GDT) and Oil Up To (OUT) was observed, then we used halfway. If only OUT was observed, then, GOC is determined by taking halfways between crest and OUT, lastly, if only GDT was observed, GOC was determined by using crest + average gas column in that particular block. The most important factor for using these workflows for determining the Fluid contacts is to choose the real " initial well" with the assumptions that the logs response were true. The 'initial wells' were then used as an anchor for saturation matching as shown in **Figure 16**.

A customized program/script was created to assign all those fluid contacts automatically in each compartment, hence enabling an automated saturation model. The script is extremely useful in shortening timeframes, especially with frequent contact updates and during uncertainty analysis exercises. The cross section which illustrate initial fluid contact complexity in Baram Field is provided in the **Figure 17**.

Property Model Results.

To validate the property model result, a blind test was conducted. Commonly, this validation was only conducted when we have extensive lateral information from secondary data (seismic). However, in case of Baram, a large number of wells were considered to sufficiently represent the lateral variation of field heterogeneity. The blind test result is very good, showing consistent profiles between log data at wells and extracted log from the 3D model (**Figure 18**).

Conclusions

A complex Giant field always poses substantial reservoir management challenges. Such fields are often associated with low recovery factors despite good reservoir quality. An integrated interdisciplinary perspective is required to properly manage and optimize the reservoir's potential.

The establishment of an integrated reservoir model for such a field is not a trivial process, especially under a constrained time frame, but still a possible task considering:
1. Continuous review and adoption of the latest available technology.
2. An Innovative project management approach.
3. Interdisciplinary communications to establish a fit for purpose modeling workflow.

The modelling work in Baram has set a new level for technology utilization and project acceleration in mature and complex field reservoir management. As demonstrated, the alignment of technical details and business objectives in managing giant fields, has now become an attainable process.

Acknowledgements

We would like to express our gratitude to the Management of Petronas Carigali Sdn Bhd (PCSB), and Petronas Petroleum Management Unit (PMU) for permission to publish this paper. Our special thanks also to Vu Quach, Khong Kheng Ting, Budi Rahim Permana, and Doan Hoang Thang who were very cooperative and dedicated to accomplishing the study.

References

Cuddy, S.J. 1998. Litho-facies and Permeability Prediction from Electrical Logs using Fuzzy Logic. Paper SPE 65411 presented at Abu Dhabi International Petroleum Exhibition and Conference, Abu Dhabi, 11-14 October 1998.

Benzaoui, K., Cox, T. 2009. Integration of Multi Scale Data in Facies Modeling using Neural Network. CSPG CSEG CWLS Convention, Calgary, Canada.

Bhatt, A., Helle, H.B. 2002. Determination of facies from well logs using modular neural networks. In Petroleum Geoscience, September 2002 v. 8 no. 3p. 217-228.

Dubois, M.K., Bohling, G.C., Chakrabarti, S. 2005. Comparison of Rock Facies Classification using Three Statistically Based Classifiers. Kansas Geological Survey, Open File Report 2004-64.

Silva, F., Ghani, A., Al-Mansouri, A., and Bahar, A. 2002. Rock Type Constrained 3D Reservoir Characterization and Modeling. Paper SPE 79504 presented at the 10th ADIPEC, Abu Dhabi, Oct 2002.

Guo, G., Diaz , M.A., Paz , F., Smalley ,J., Waninger, E.A. Rock Typing as an Effective Tool for Permeability and Water-Saturation Modeling: A Case Study in a Clastic Reservoir in the Oriente Basin. Presented in SPE ATCE, 9-12 October 2005, Dallas, Texas.

Hoffman, K.S., Neave, J.W., Nilsen, E.H. Model Building with Difficult Faults. Paper SPE 115324 presented in SPE ATCE, 21-24 September 2008, Denver, Colorado.

Hoffman, K.S., Neave, J.W., Nilsen, E.H. Building a Reservoir Model with Problematic Faults. Paper SPE 110367 presented in SPE Western Regional and Pacific Section AAPG Joint Meeting, 31 March - 2 April 2008, Bakersfield, California.

Aly, A., Lee, W.J., Datta-Gupta, A., Mowafi, K., Prida, M., Latif, M. Application of geostatistical modeling in an integrated reservoir simulation study of the Lower Bahariya reservoir, Egypt. Paper SPE presented in SPE Middle East Oil Show and Conference, 1999, Bahrain.

Choo, C.F. State of the Art Permeability Determination from Well Logs to Predict Drainage Capillary Water Saturation in Clastic Rocks. Paper presented in SPWLA 51st Annual Logging Symposium, 19-23 June 2010, Perth, Australia.

SIEP internal report, Various Authors. Baram Redevelopment Field Development Plan, June 2008.

SIEP internal report, Various Authors. Baram Full Field Review Phase 1 Report, November 2006.

SIEP internal report, Various Authors. Baram Improved Recovery Factor Report, March 2006.

SIEP internal report, Various Authors. Petrophysical study of Baram field, Baram Delta Operations, Sarawak, Malaysia, October 2005.

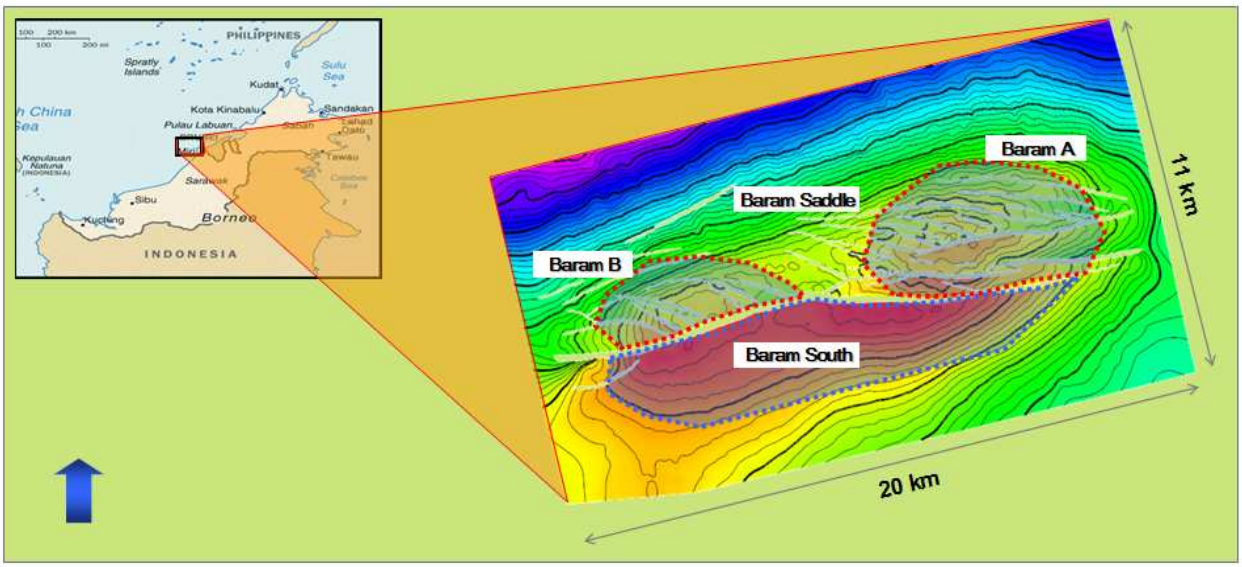

Figure 1 : Location and outline of Baram Field

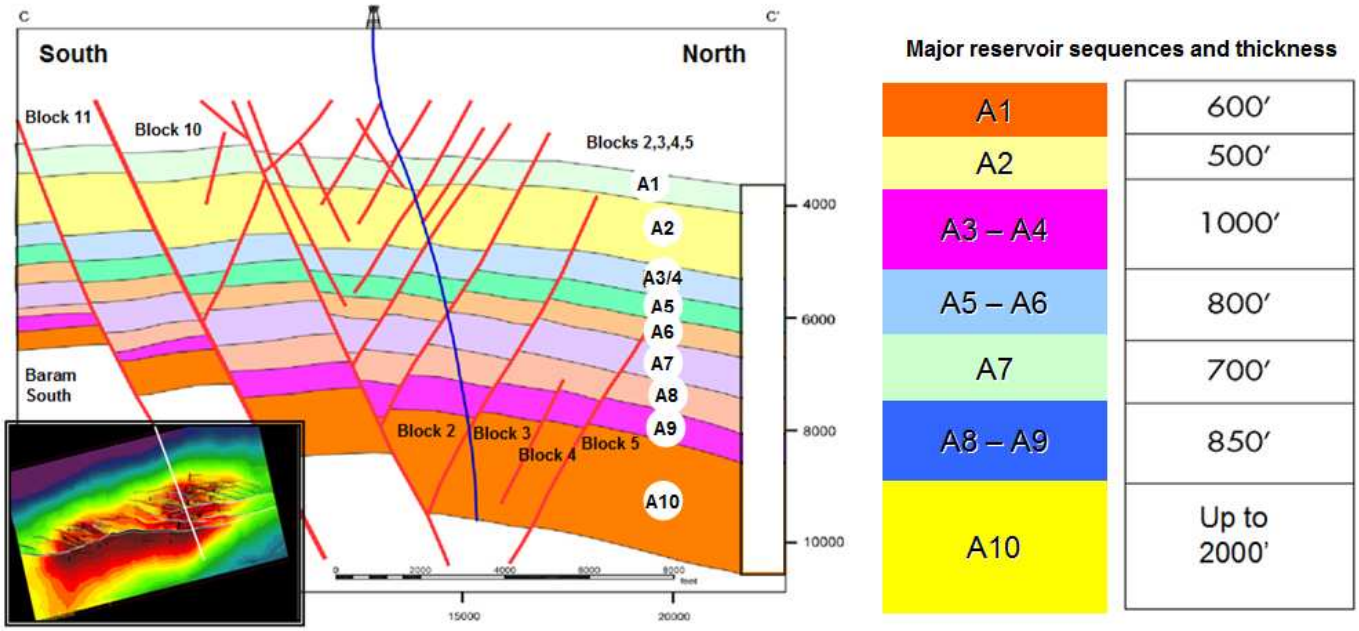

Figure 2. Baram Field reservoir unit cross section and approximate thickness

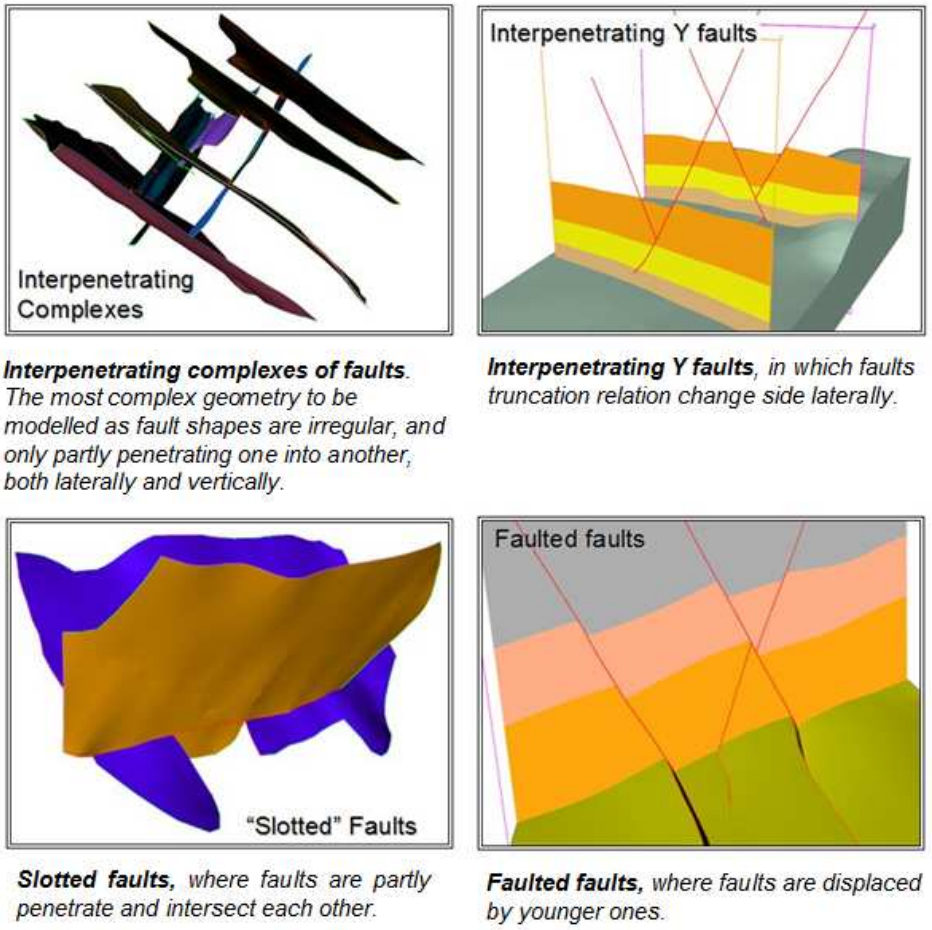

***Interpenetrating complexes of faults**. The most complex geometry to be modelled as fault shapes are irregular, and only partly penetrating one into another, both laterally and vertically.*

***Interpenetrating Y faults**, in which faults truncation relation change side laterally.*

***Slotted faults,** where faults are partly penetrate and intersect each other.*

***Faulted faults,** where faults are displaced by younger ones.*

Figure 3. Examples of the challenging geometry of faults in the Baram Field

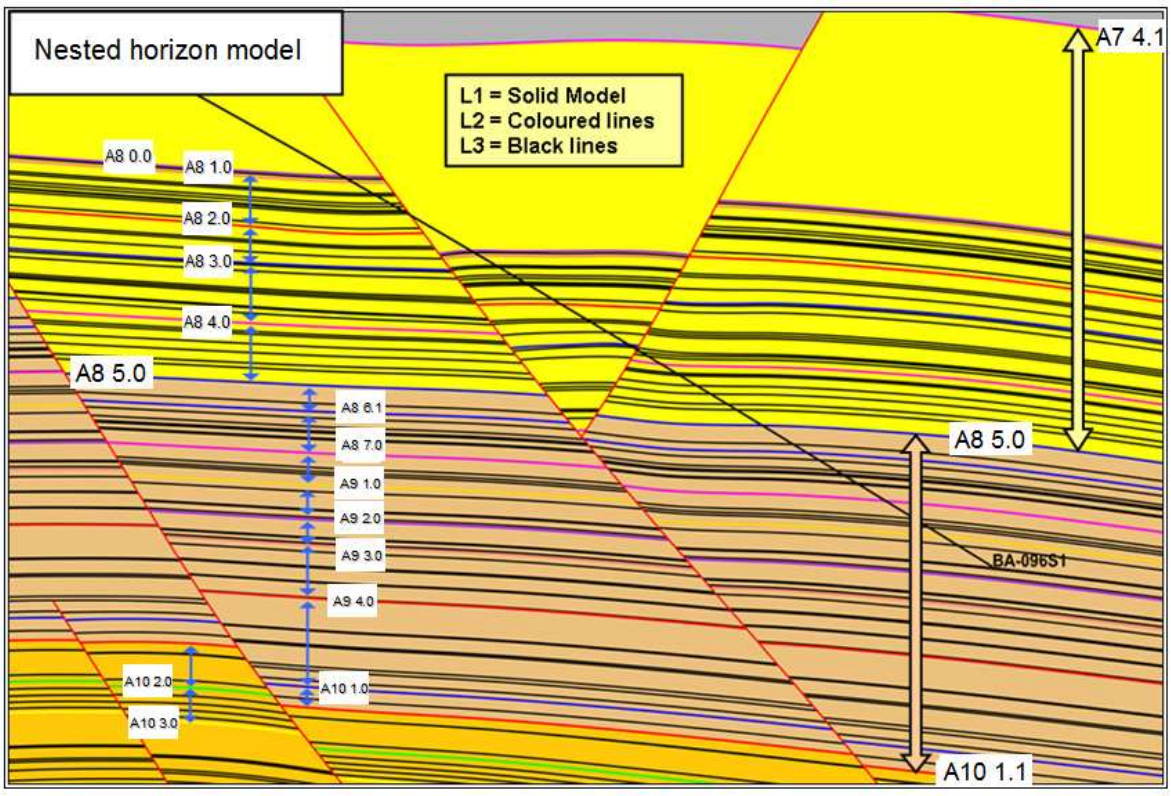

Figure 4. Illustration of the nested horizon model framework

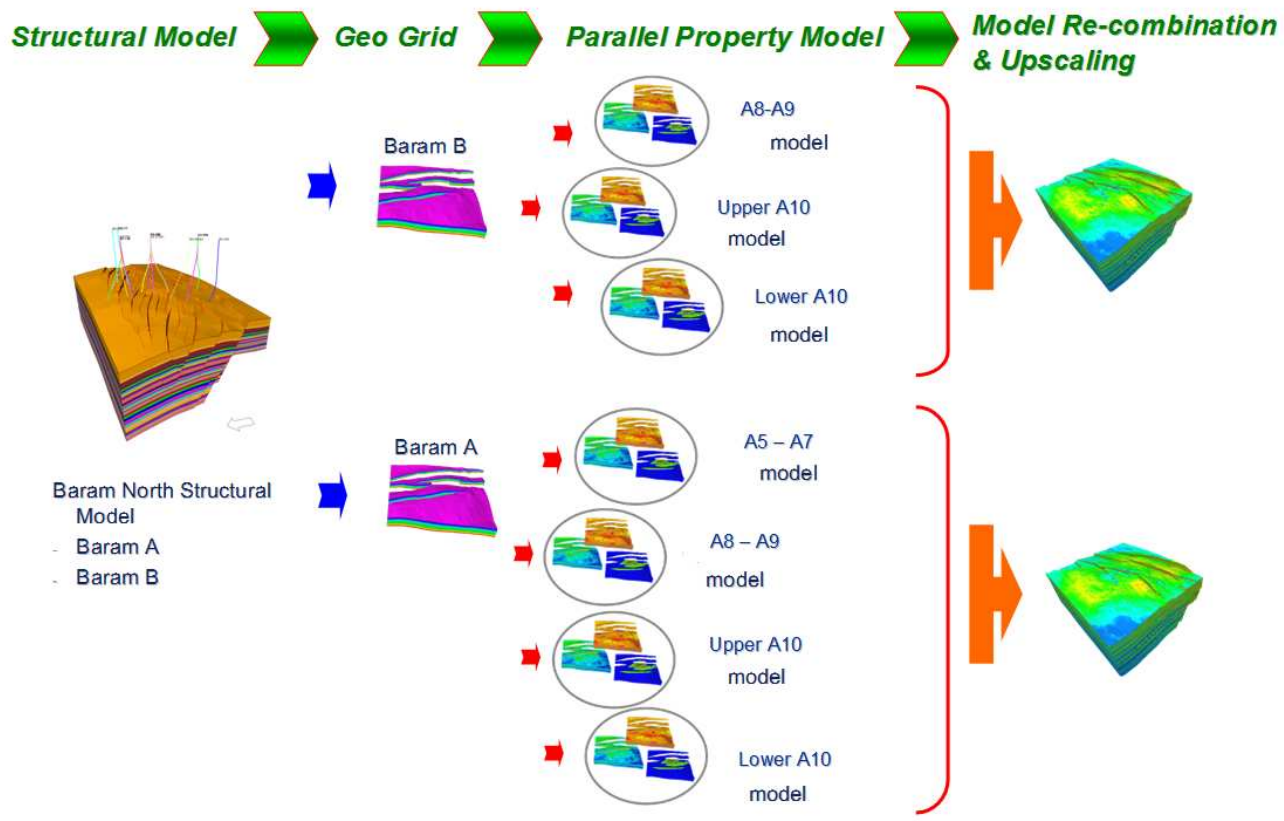

Figure 5. Diagram of the parallel property modeling process, key-stratigraphic grid split, parallel property population, and integration back into an integrated simulation grid

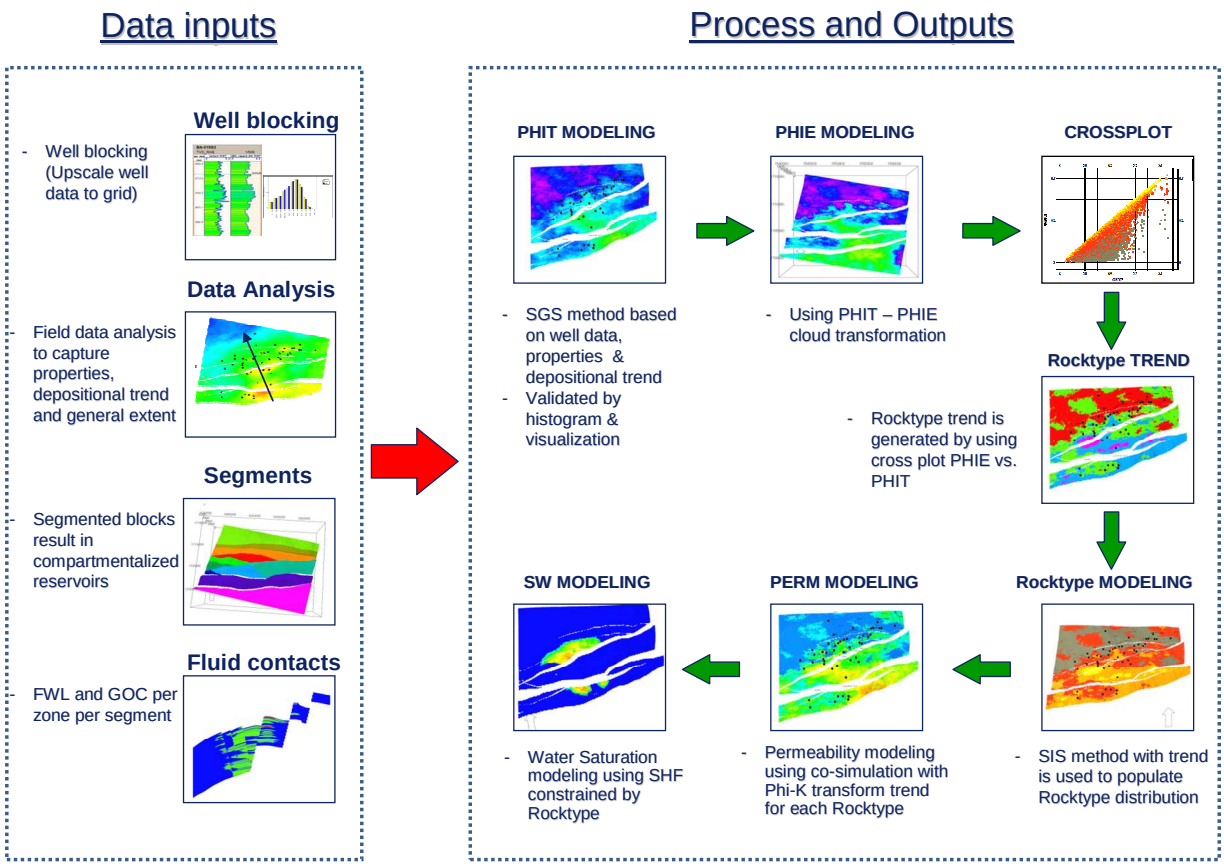

Figure 6. A common, high-level property modeling workflow used in the Baram static model

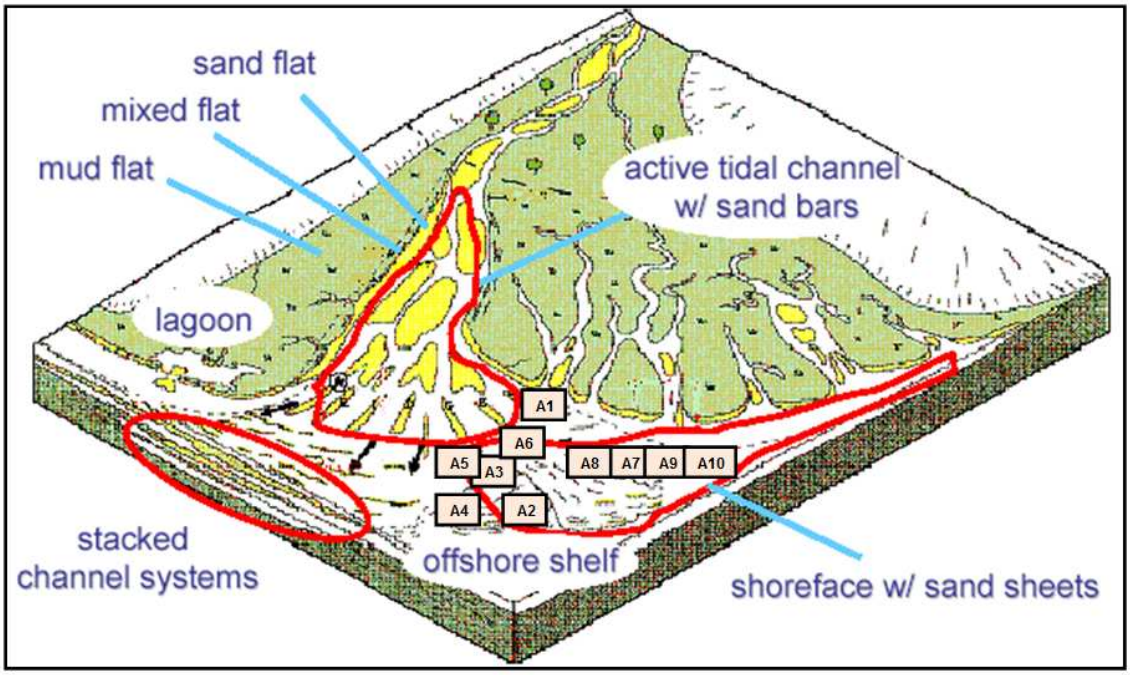

Figure 7. The Baram reservoirs depositional system conceptual model

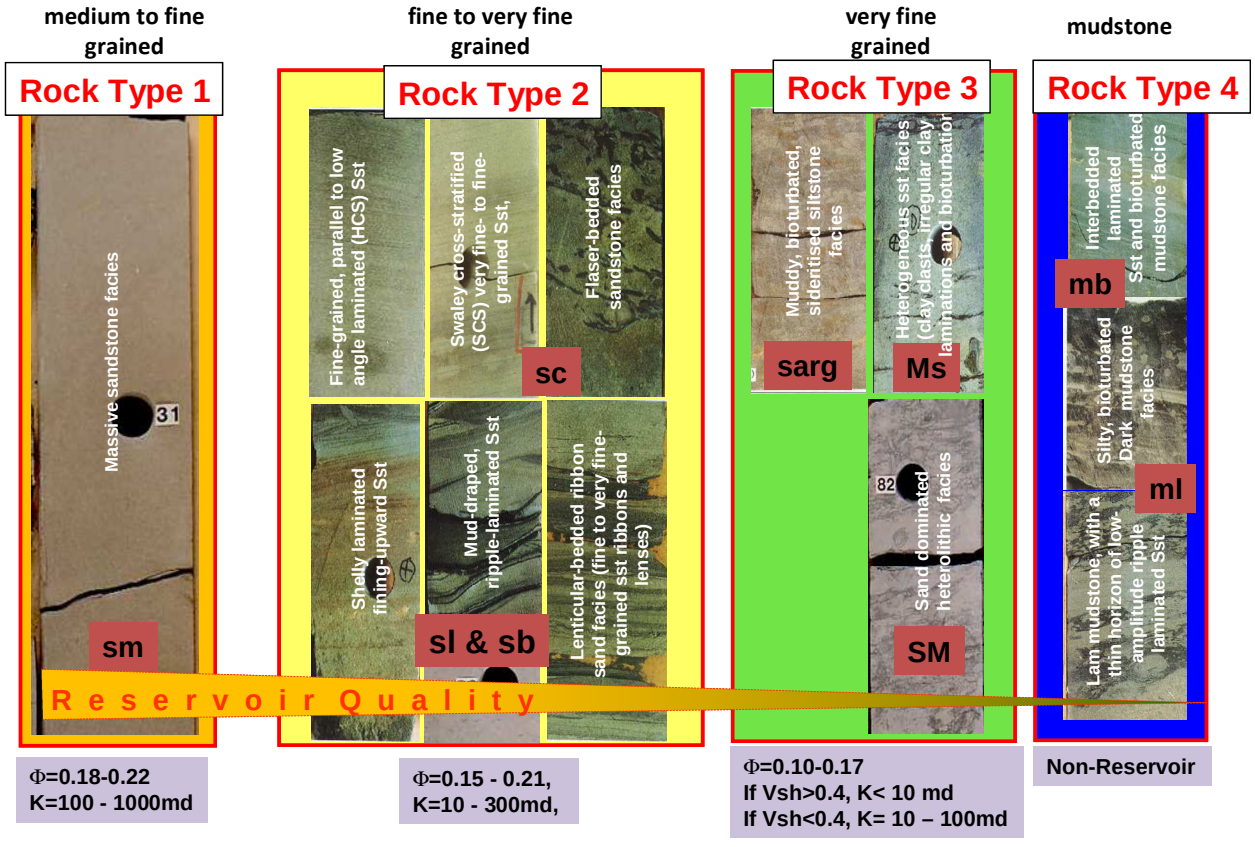

Figure 8. Core lithology grouping into four rock types.

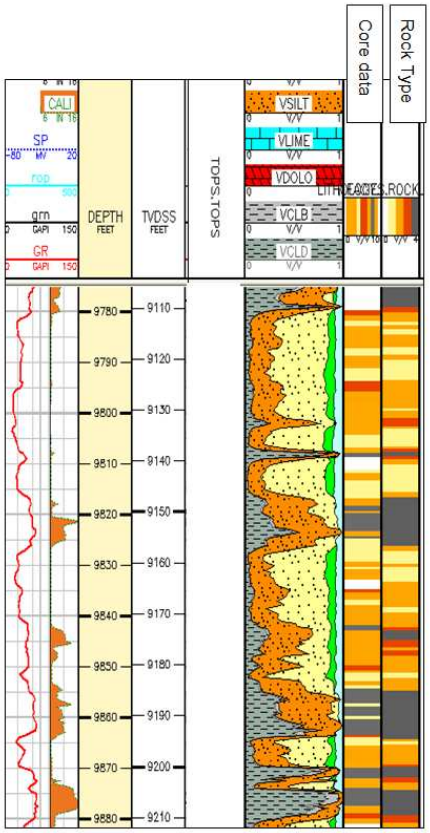

Figure 9. Comparison of core vs log-derived rock type

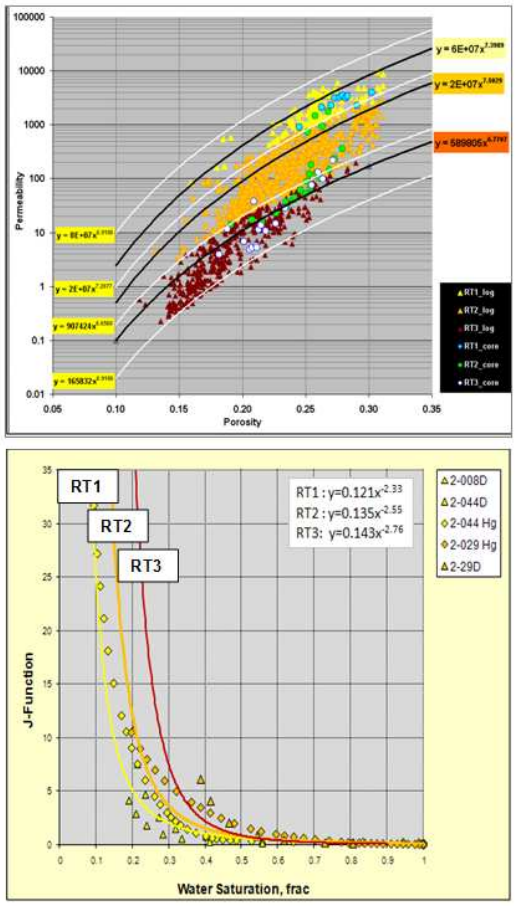

Figure 10. Poro-perm and Saturation height function eq. for as defined for each rock type

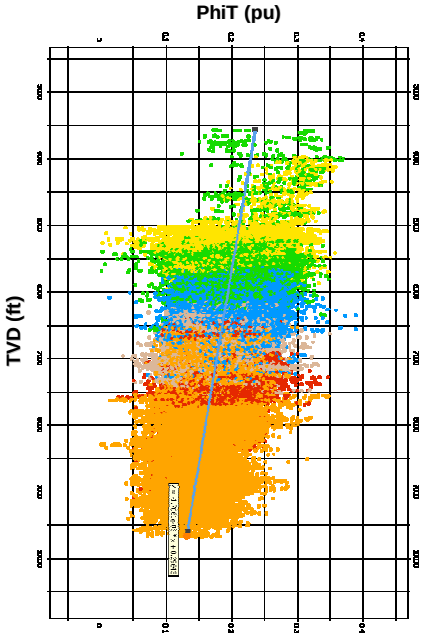

Figure 12. Compactional trend of total porosity (Phit) observed from well data

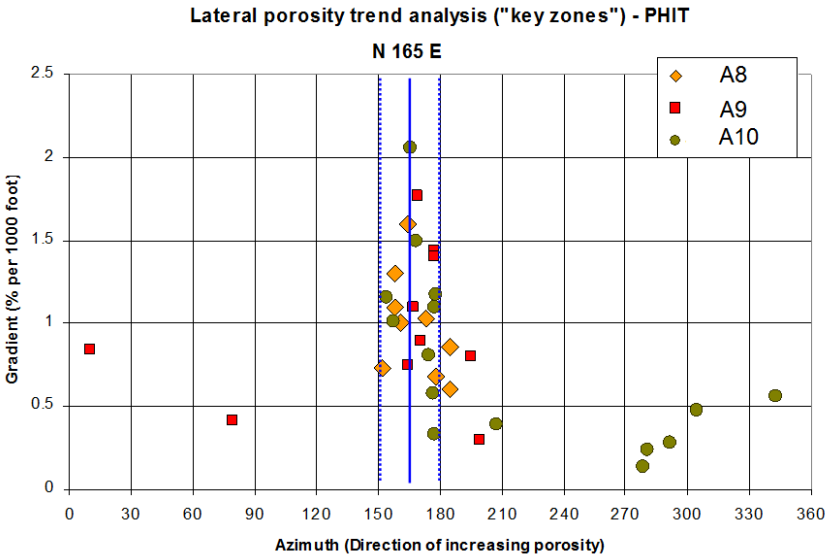

Figure 11. Porosity lateral trend extraction from Baram wells

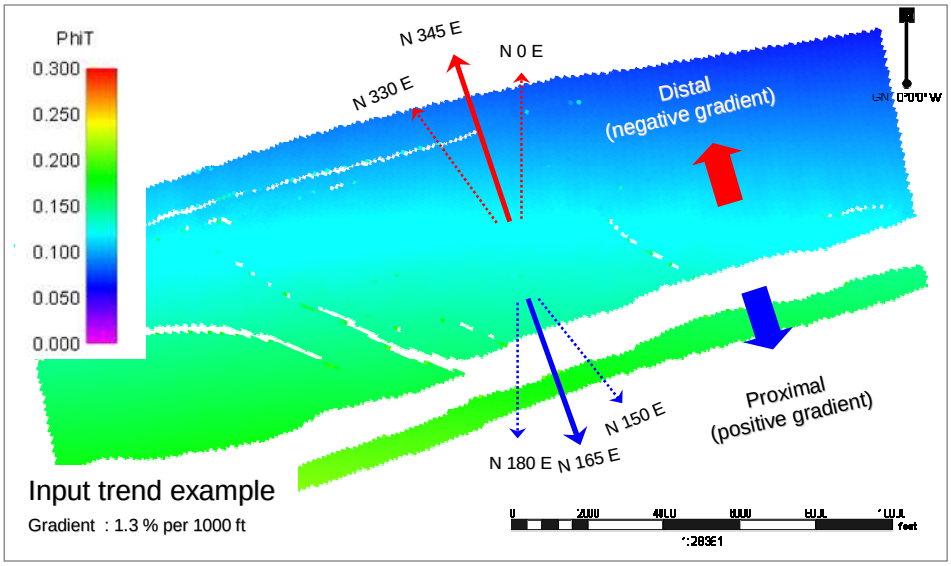

Figure 13. Example of porosity trend extracted from wells at a specific horizon.

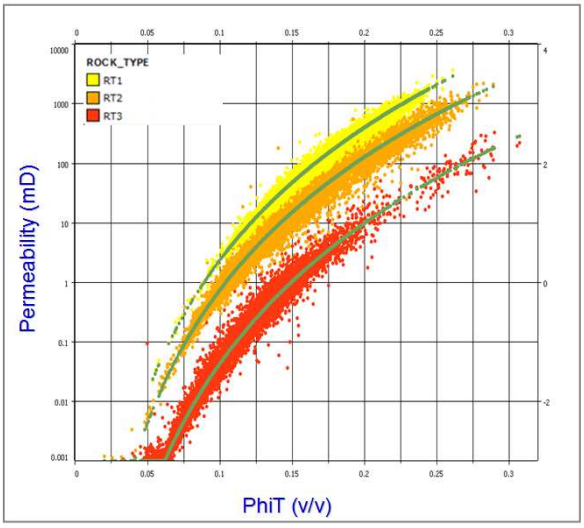

Figure 14. Poro - perm 3D model cross plot

No	OIL - WATER interface		Coverage
	Event	FWL determination	(%)
1	OWC observed from Logs	Extrapolate OWC to FWL using SHF	*5*
2	Good saturation profile from logs	Estimate FWL using SHF	*82*
3	Logs saturation profile could not be matched using SHF (Distance ODT to WUT : small ~ < 30 ft)	Vertical mid-point of ODT to WUT	*10*
4	Logs saturation profile could not be matched using SHF (Distance ODT to WUT : big ~ > 30ft)	GOC + average oil column height in the particular reservoir	*3*

No	GAS - OIL interface		Coverage
	Event	GOC/FOL determination	(%)
1	GOC observed from Logs	GOC	*5*
2	GDT and OUT observed from logs	Vertical mid-point between GDT to OUT	*25*
3	Only OUT observed from logs	Vertical mid-point between Crest to OUT	*60*
4	Only GDT observed from logs	Crest + average gas column height in the particular reservoir	*10*

Table 1. Fluid contact determination methodology

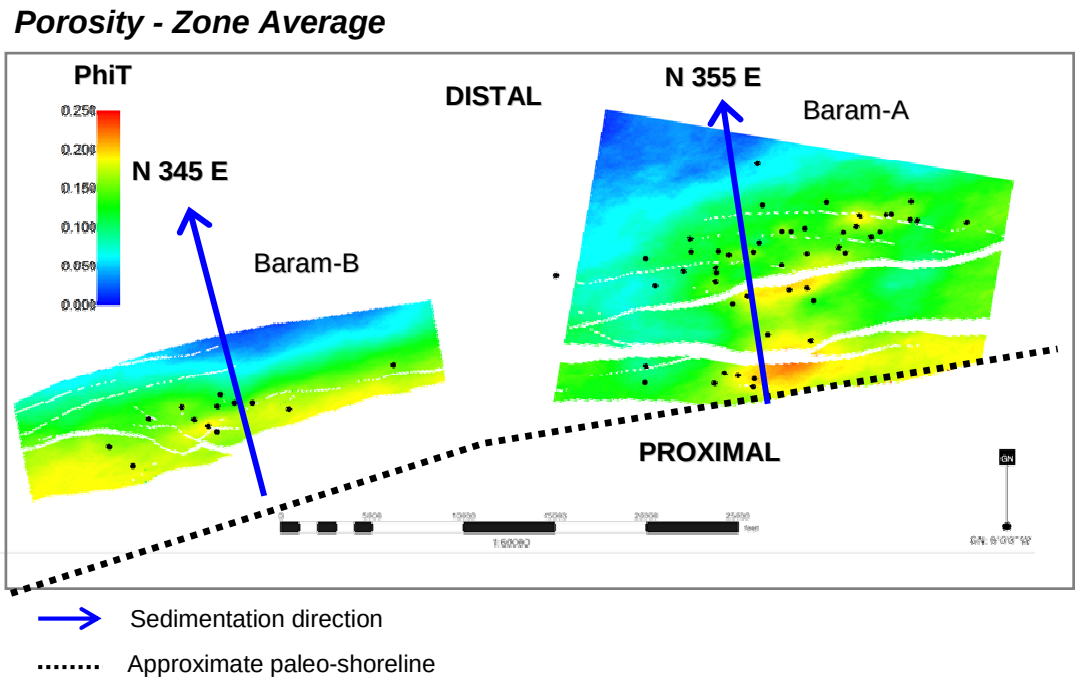

Figure 15. Property model (Phit) result, demonstrating a good representation of a shoreface geological system. Good continuity along shoreline with some disturbed trend indicating tidal process (NE of Baram A).

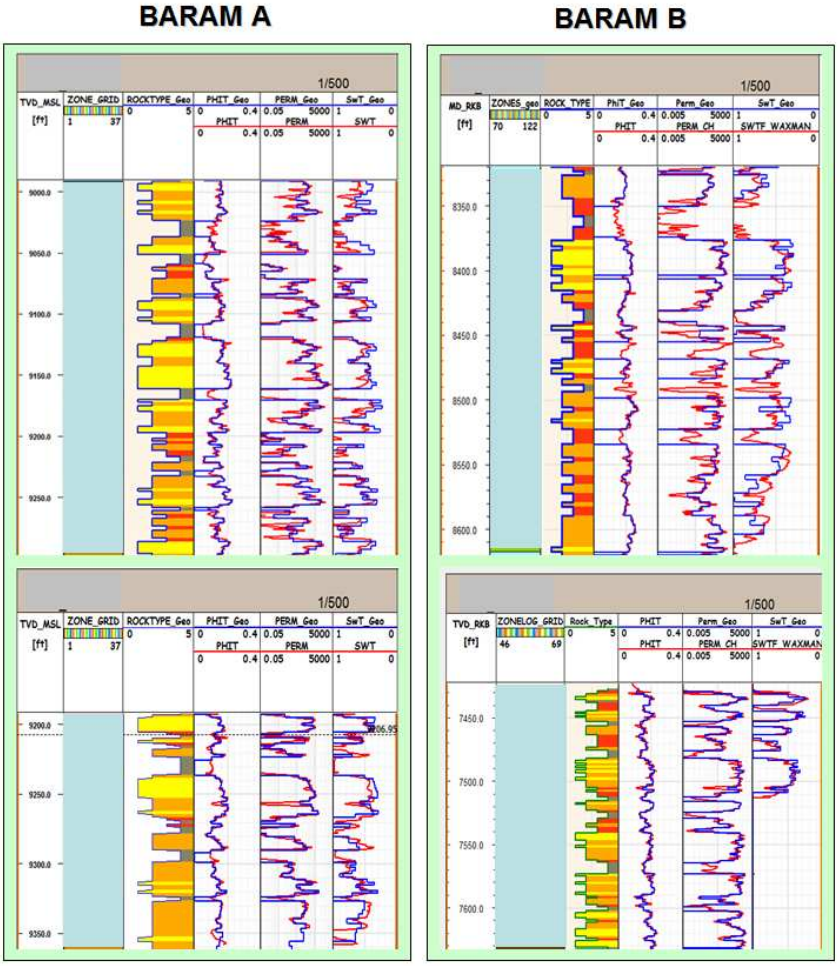

Figure 16. Saturation matching profile at representative well in Baram A and B. Red curve is original log while blue curve shows extraction of 3D model.

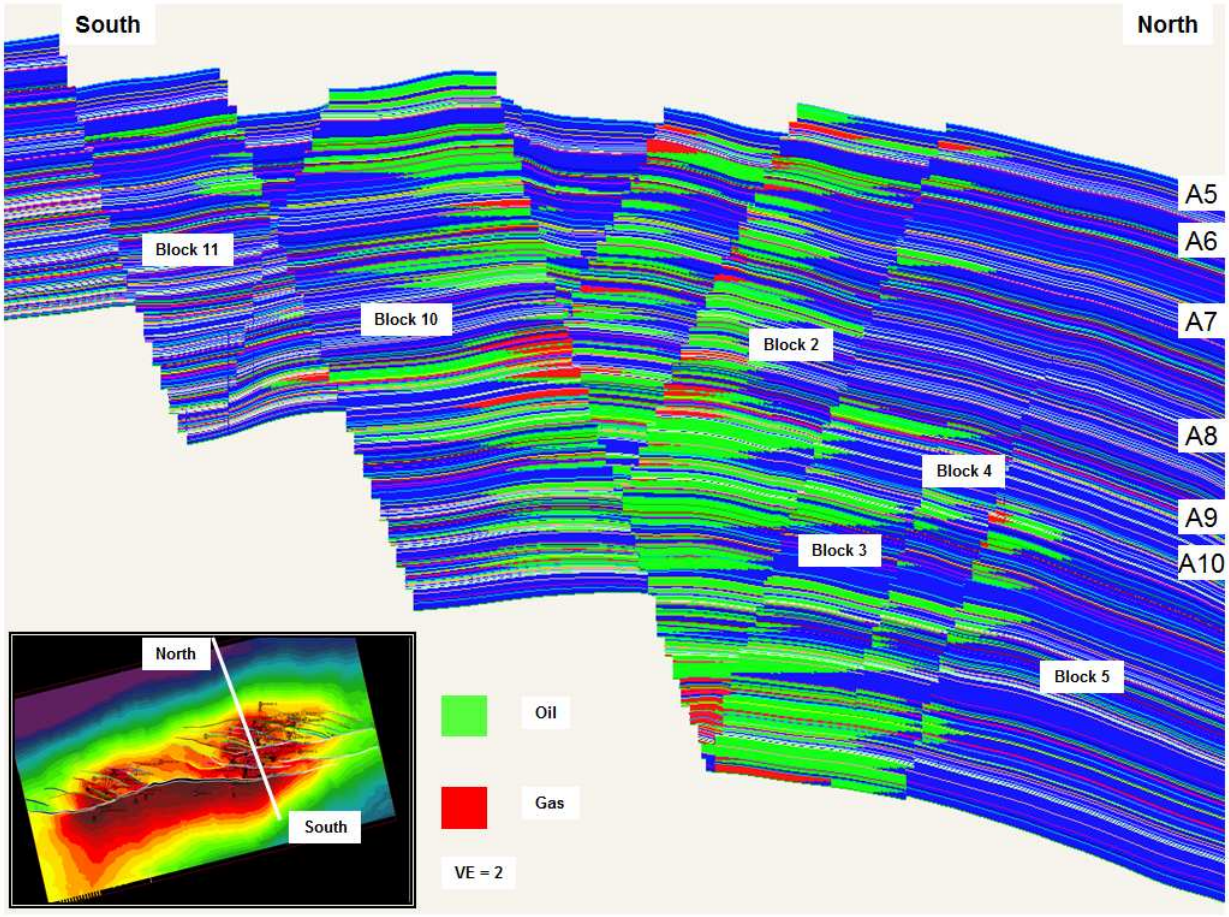

Figure 17. Dip-line cross section of Baram Initial fluid contacts in A5, A6, A7, A8, A9, and A10 reservoirs

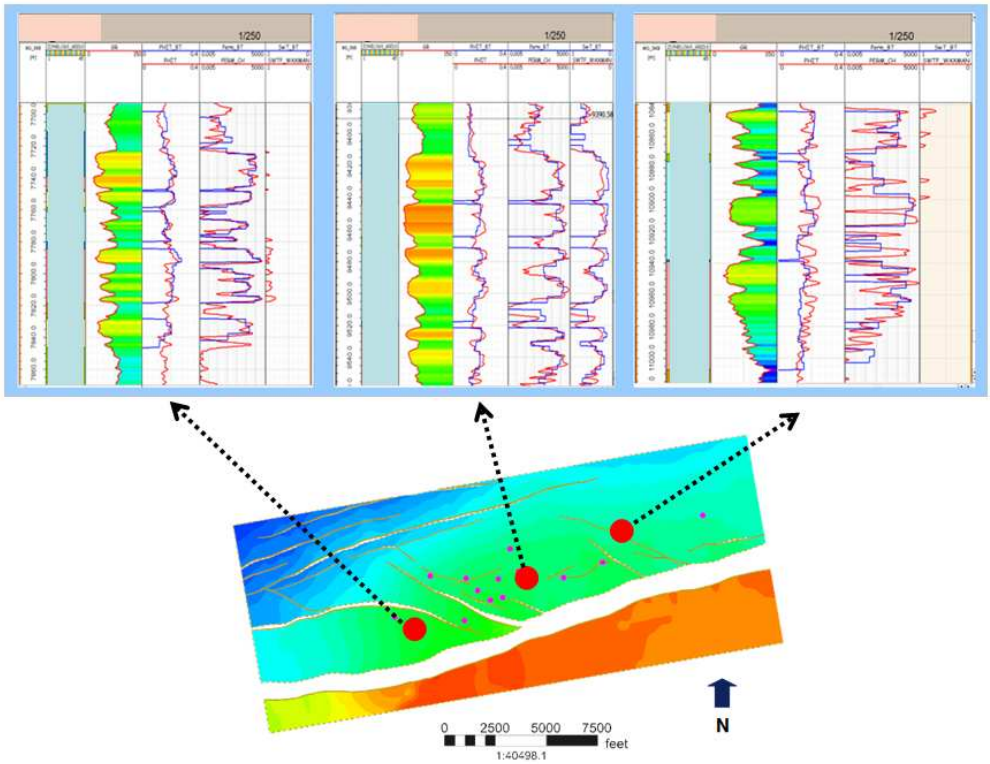

Figure 18. Blind test result on three wells at dispersed locations showing consistency between well data and model results.